Contents list available at IJRED website

International Journal of Renewable Energy Development

Journal homepage: https://ijred.undip.ac.id

Research Article

QPVA-Based Electrospun Anion Exchange Membrane for Fuel Cells

Asep Muhamad Samsudin [a,b*] and Viktor Hacker [a]

[a] *Institute of Chemical Engineering and Environmental Technology (CEET), Graz University of Technology, Austria*

[b] *Department of Chemical Engineering, Diponegoro University, Indonesia*

Abstract. The anion exchange membrane is one of the core components that play a crucial and inseparable role in alkaline anion exchange membrane fuel cells. Anion exchange membranes (AEMs) were prepared from quaternary ammonium poly(vinyl alcohol) (QPVA) by an electrospinning method. QPVA was used both as material for electrospun fiber mats and as filler for the inter-fiber void matrix. The objective of this work is to investigate the influence of the inter-fibers void matrix filler concentration on the properties and performance of eQPVA-x AEMs. FTIR spectra were used to identify the chemical structures of the AEMs. The primary functional groups of PVA and quaternary ammonium-based ion conducting cation were detected. The surface morphology of QPVA nanofiber mats and eQPVA-x AEMs was observed using SEM. Electrospun nanofiber structures of QPVA with an average size of 100.96 nm were observed in SEM pictures. The ion exchange capacity, swelling properties, water uptake, and OH^- ions conductivity were determined to evaluate the performance of eQPVA-x AEMs. By incorporating the QPVA matrix of 5 wt.% concentration, the eQPVA-5.0 AEMs attained the highest ion exchange capacity, water uptake, swelling properties, and OH^- conductivity of 0.82 mmol g^{-1}, 25.5%, 19.9%, and 2.26 m·s cm^{-1}, respectively. Electrospun QPVA AEMs have the potential to accelerate the development of alkaline anion exchange membrane fuel cells.

Keywords: anion exchange membranes, fuel cells, QPVA, electrospinning, nanofibers

Received: 30th Oct 2022; Revised: 2nd January 2023; Accepted: 29th January 2023; Available online: 11th February 2023

1. Introduction

The decline of energy reserves and the occurrence of ecological damage encourage researchers to develop renewable energy sources that are more environmentally friendly, efficient, and sustainable. Efforts to produce electrical energy from mechanical, thermal, and chemical energy have continued in the last few decades (Ayaz *et al.*, 2022).

Among the developed new energy sources, the fuel cell is regarded as eco-friendly alternative energy that can replace conventional fossil fuels with high efficiency of energy conversion and almost no emissions. Anion exchange membrane fuel cells (AEMFCs), as one fuel cell category, are getting immense attention because of their advantages. The advantages include the opportunity to utilize less expensive transition metals instead of a costly catalyst of platinum group metals (PGM) and a faster oxygen reduction process. Due to the counter-direction between the fuel and OH^- ions, AEMFCs also benefit from reduced fuel crossover and reduced corrosion concerns in alkaline environments (Iravaninia & Rowshanzamir, 2015; Samsudin *et al.*, 2022).

Anion exchange membranes (AEMs) are part of a fuel cell that has an essential role in hydroxide conduction, electron inhibition, and gas barrier (Hagesteijn *et al.*, 2018; Ramaswamy & Mukerjee, 2020). Despite their positive points, the development of AEMFCs faces several difficulties. Since hydroxide ions have lower mobility than hydrogen ions, the ionic conductivity of AEMs tends to be lesser than that of proton exchange membranes (PEMs) (Das *et al.*, 2022). The toxic and expensive solvents are also an issue in the synthesis of some AEMs. In addition, complex routes and costly equipment have also become a concern (Wang *et al.*, 2013).

Polymers are the backbone material used in the manufacture of AEMs. To date, many types of polymers have been developed for AEMs, ranging from poly (aryl ether) based AEMs (e.g., poly (ether sulfone) (Du *et al.*, 2022; Wang *et al.*, 2022), poly(2,6-dimethyl-1,4-phenylene oxide)(Becerra-Arciniegas *et al.*, 2019; Mayadevi *et al.*, 2022) and aryl-ether free AEMs (e.g., polybenzimidazole (Guo *et al.*, 2022; G. Zhang *et al.*, 2022) and aliphatic-based AEMs (e.g., poly (vinyl alcohol) (Huang *et al.*, 2022; Samsudin & Hacker, 2019, 2021).

Poly(vinyl alcohol) (PVA) is a synthetic polymer that possesses scentless, flavorless, biocompatible, and biodegradable characteristics. Due to its beneficial attributes, PVA is frequently employed as a backbone polymer for AEMs development. Due to its hydrophilicity, it exhibits a high water uptake and possesses exceptional film-forming characteristics. Furthermore, the availability of reactive functional groups and lesser fuel crossover are favorable for chemical crosslinking and other modifications that improve the properties of the membrane (Aslam *et al.*, 2018; Ding & Qiao, 2022; Samsudin *et al.*, 2022; Susanto *et al.*, 2016; Zhang *et al.*, 2013).

Various techniques and methods for membrane preparation of functionalized polymers have been introduced. Solution casting is a membrane casting technique that has been widely used because it is simple, easy, and versatile (Samsudin *et al.*, 2022). Apart from solution casting, another method that is starting to attract attention is electrospinning. This technique employs a high-voltage source to induce an electric field from

* Corresponding author
Email: asep.samsudinl@live.undip.ac.id (A.M. Samsudin)

https://doi.org/10.14710/ijred.2023.49909
ISSN: 2252-4940/© 2022.The Author(s). Published by CBIORE

the spinneret to the collector. A Taylor cone emerges at the spinneret's edge at a particular electric field intensity. After intensity overcomes polymer drop surface tension, an electrified solution jet is released from the Taylor cone. The solution jet evaporates and solidifies in the collector, forming nanofibers (Sood *et al.*, 2016). Electrospinning is favorable because it facilitates the formation of interlinked structures, which improves OH^- transfer. Additionally, electrospinning is effective for achieving a uniaxial alignment of nanofiber-formed polymer chains that has the potential to strengthen the membrane (Fennessey & Farris, 2004; Sood *et al.*, 2016; Tamura & Kawakami, 2010).

Despite the many benefits, the fabrication of anion exchange membranes by electrospinning is still limited. Yang *et al.* prepared electrospun AEMs, which utilized a combination of poly(vinyl alcohol) and chitosan. They investigated the impact of various crosslinking times on the characteristics of the membrane (Yang *et al.*, 2018). Gong *et al.* compared imidazolium-functionalized polysulfone (IMPSF) AEMs manufactured by the solution casting and electrospinning methods. The results depict that electrospun AEMs produce higher conductivity and lower swelling properties than cast membranes (Gong *et al.*, 2016). Du *et al.* fabricated quaternized poly(2,6-dimethyl-1,4-phenylene oxide) electrospun (QPPONF)/poly(vinyl alcohol) anion exchange membrane. By varying the ratio between QPPONF and PVA, it was found that the addition of the ratio of QPPONF to PVA increased the ion conductivity of AEMs (Du *et al.*, 2020).

Most developments in the field of electrospun anion exchange membranes have concentrated on nanofiber mats, while studies on matrix fillers are still rare. In this work, QPVA-based electrospun nanofiber AEMs were prepared by an electrospinning method. A commercially available QPVA, namely Gohsenx™ K-434, was used for both the fibers and the matrix filler between the fibers. The objective of this work is to study the influence of different concentrations of QPVA as inter-fibers void matrix fillers on the AEMs properties.

2. Experimental

2.1 Preparation of Electrospun AEMs

12 wt.% of QPVA solute was prepared by dissolving QPVA (Gohsenx™ K-434, 85.5-88.0% hydrolyzed, 18-22 mPa.s, obtained from Mitsubishi Chemical Corporation) in ultrapure water (UPW, resistivity ~18 MΩ.cm) with constant stirring at 80–90 °C overnight. The chemical structure of Gohsenx™ K-434 is depicted in Figure 1. A quantity of the QPVA solution was then inserted into a 10 mL size spinneret needle syringe. A horizontal movable spinneret and a drum collector which a distance of 10 cm were used to increase the dimensional homogeneity of the membrane. Then, 20 kV high voltage was introduced between the spinneret edge and the aluminium foil-coated drum collector. The electrospinning was carried out with a polymer flow rate of 0.5 mL/h at room temperature. The relative humidity was set in the range of 50–60%. The QPVA fiber mats were heated at 130 °C for one hour to induce physical crosslinking between QPVA polymer chains. Subsequently, they were soaked in a cross-linker solution composed of 2.5 wt.% glutaraldehyde, 0.2 wt. % hydrochloric acid in acetone to promote chemical crosslinking. To produce dense AEMs (QPVA-x), QPVA Fiber mats were then submerged in various concentration of Gohsenx™ QPVA solution at room temperature. Then, crosslinking was repeated for AEMs to increase crosslinking degree QPVA chains. The identities of the QPVA AEMs were determined using Table 1. The AEM's preparation processes are shown in Figure 2.

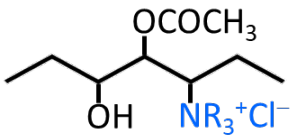

Fig. 1 The structure of GOHSENX™ K-434

Table 1
The AEMs samples composition

Membrane Samples	Fiber (QPVA) (wt.%)	Matrix Filler Concentration (QPVA) (wt.%)
cQPVA	12	-
eQPVA-2.5	12	2.5
eQPVA-5.0	12	5.0
eQPVA-7.5	12	7.5
eQPVA-10.0	12	10.0

2.2 FTIR Analysis

An IR-Bruker ALPHA spectrometer was used for the FTIR study to determine the major functional group of the membranes. FTIR analysis was conducted at a wavenumber of 400–4000 cm^{-1} and a resolution of 4 cm^{-1}. The IR spectra of the AEMs were displayed as absorbance versus wavenumber graphs.

2.3 SEM Analysis

SEM analysis (Zeiss Supra 55VP) was conducted to study the morphology of the electrospun QPVA AEMs. The measurement was performed at a voltage of 15 kV. The nanofiber size distribution of the electrospun mats was determined using ImageJ software on SEM results.

2.4 Ion Exchange Capacity (IEC)

The IEC of eQPVAx AEMs was measured by back titration. Firstly, the membranes were weighed and then soaked for 24 h in 1 M KOH solution to change the AEMs into OH^- form. After removing the KOH residue using ultra-pure water for 24 h, the AEMs samples were then soaked for 24 h in 0.1 M HCl solution. The titration was accomplished using 0.1 M KOH solution. IEC was calculated using Formula 1 (Samsudin *et al.*, 2022) as follows:

$$\mathrm{IEC} = \frac{(\mathbf{V_b} - \mathbf{V_m}).\mathbf{C_{HCl}}}{\mathbf{w_d}} \quad (1)$$

where, V_b, V_m, C_{HCl}, and W_d are the consumed KOH volumes of the 0.1 HCl solution without membrane samples, the consumed KOH volumes of AEMs, the HCl concentration, and the dry weight of AEMs, respectively.

2.5 Swelling Properties

The AEMs' swelling properties were assessed by measuring water uptake (WU) and swelling degree (SD). The WU was measured by determining the weight difference of the AEMs after submerging them in water. On the other hand, the SD was evaluated by comparing the volume of AEM due to water immersion for 24 h in RT. Formula 2 and 3 (Movil *et al.*, 2015) were used for calculating the WU and SD as follows:

$$\mathrm{WU} = \frac{W_w - W_d}{W_d} \times 100\% \quad (2)$$

$$\mathrm{SD} = \frac{V_w - V_d}{V_d} \times 100\% \quad (3)$$

where, W_w, W_d, V_w, and V_d are the wet weight, dry weight, wet volume, and dry volume of AEMs, respectively.

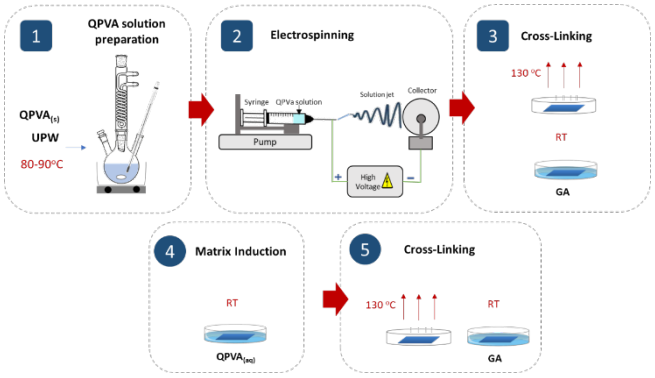

Fig. 2 Schematic of the preparation procedure

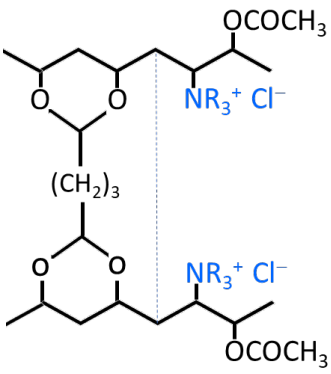

Fig. 4 Chemical structure of crosslinked QPVA

2.6 Ion Conductivity

Electrochemical impedance spectroscopy was utilized to evaluate ionic conductivity (σ). The Gamry Reference 600 potentiostat was used in conjunction with a standard four-probe conductivity clamp (Scribner Associates, USA). The impedance of OH^- form AEMs was measured between 0.1 Hz and 10 kHz frequency and with 50 mV voltage. Formula 4 (Feketefoldi & Cermenek, 2016) was used for calculating the σ as follows:

$$\sigma = \frac{d}{R_m.T.W} \quad (4)$$

Where d, R_m, T, and W are the distance of electrodes, the impedance of membranes, the thickness of wet AEMs, and the width of the membranes, respectively.

3. Results and Discussion

3.1 Chemical structure of AEMs

FTIR spectroscopy was used to verify the chemical composition of eQPVA-x AEMs. Figure 3 displays the FTIR spectra of eQPVA-x AEMs. The absorption peaks at 3378 and 1022 cm^{-1} appear to be caused by the –OH and C–O stretch in the PVA polymer backbone. The peak in the bending vibration at 2940 cm^{-1} attributable to the existence of the C–H group. The stretching vibration of the chemical bond C=O was indicated by the intensity at the wavenumber of 1734 cm^{-1}. The intensity at 1434 cm^{-1} and 1376 cm^{-1} occur on account of the presence of the CH_3 bend and CH_2 bend, respectively. A wavenumber of 1240 cm^{-1} belongs to the C–O–C bond stretching vibration, which indicates the establishment of covalent bonds between –OH groups of QPVA and –CHO groups from GA.

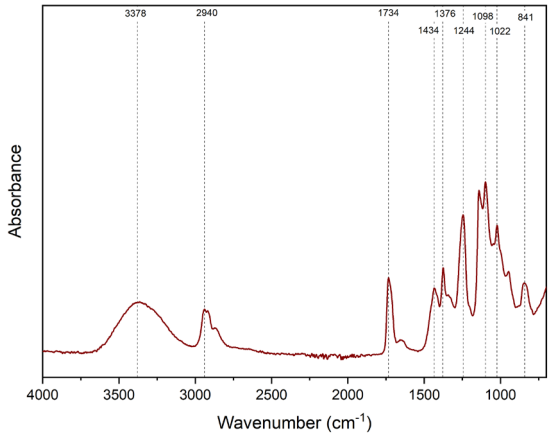

Fig. 3 FTIR Spectrum of eQPVA-5.0

The intensities at 1098 cm^{-1} and 841 cm^{-1} correspond to the C–N stretch and N–H bend of ion-conducting cation groups in QPVA. The chemical structure of crosslinked QPVA is illustrated in Figure 4.

3.2 Morphology

Figure 5a shows the surface morphology of the eQPVA nanofiber AEMs from the SEM analysis. It was seen that the nanofibers formed well with no beads. The size distribution of the nanofiber mat is presented in Figure 5b. The QPVA mats fibers possess a size distribution of 69–179 nm and a mean fiber diameter of 100.96 nm, identifying them as nanofibers (Patel *et al.*, 2018). Inter-fiber void space, visible as pores between fibers, is observed in the membranes. This inter-fiber void space of the membrane should be occupied with a matrix filler in order for it to be utilized in fuel cells.

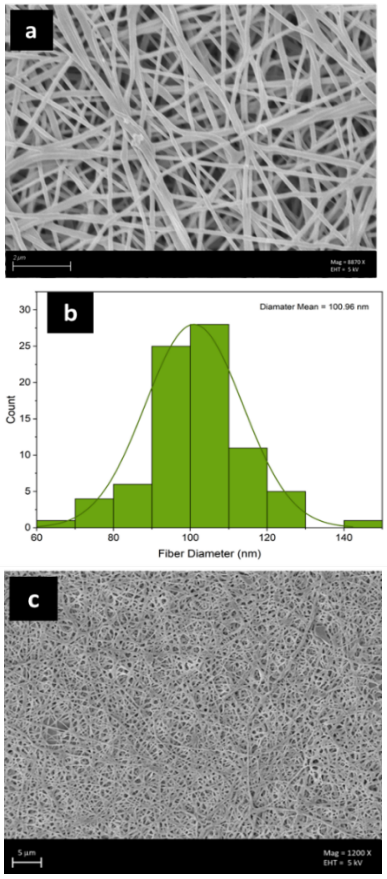

Fig. 5 a) SEM Image of QPVA nanofibers, b) QPVA nanofibers size distribution, c) SEM Image of eQPVA-5 AEM

This matrix filler can prevents fuel and oxidant gas transport through the membrane (i.e., gas crossover). The permeability of fuel through AEMs should be prevented for fuel cells. Since this crossover process may lead to voltage loss on account of the mixed potential caused by the penetrated fuel oxidation. Additionally, fuel crossover could cause peroxide and excess heat generation, which can degrade the fuel cell (Francia *et al.*, 2011; T. Huang *et al.*, 2022; Inaba *et al.*, 2006). Figure 5c shows the eQPVA-5.0 AEMs. Since this membrane is derived from matrix addition to the eQPVC nanofibers, we can see that the inter-fiber voids are filled with the matrix while maintaining the nanofiber structure.

3.3 Ion Exchange Capacity (IEC)

IEC can be described as the capability of the AEMs functional groups to carry out ions displacement, which is integrated and loosely attached to its polymer backbone chain structure by oppositely charged ions in the adjacent solution (Elumalai *et al.*, 2018). IEC demonstrates the quantity of functional groups or active sites in an anion exchange membrane that is accountable for ion exchange or facilitates the transfer of hydroxide (Kumar *et al.*, 2018). IEC can be expressed as milliequivalent or millimoles of anionic-exchange groups per gram of the dry membrane (meq g^{-1} or mmol g^{-1}).

Figure 6 depicts the ion exchange capacity (IEC) of eQPVA-x AEMs in hydroxide form of AEMs at 30°C. The IEC of eQPVA-2.5 AEMs is 0.46 mmol g^{-1}. The ion exchange capacity increases by around 78% after enhancing the concentration of the QPVA matrix to 5 wt.% (eQPVA-5.0), which is the highest IEC value. When the concentration of the QPVA matrix is enhanced to 7.5 and 10 wt.%, the IEC decreases to 0.79 and 0.41 mmol g^{-1}. The decrease of IEC at higher concentrations of the QPVA matrix is possibly owing to the QPVA matrix high viscosity, which causes an impediment for the matrix filler solution to infiltrate the inter-fiber space of the nanofiber mats. Consequently, the number of ion-conducting cations in the electrospun QPVA AEMs decreases, followed by the decline of IEC.

3.4 Swelling Properties

The existence of water in the anion exchange membranes is significant in the process of conducting hydroxide ions. The ion movement process in AEMs is highly reliant on the membrane's hydration level (λ, i.e., the water molecules number per OH^-), the dispersion and distribution of water, and the solvation of OH^- ions (Zelovich *et al.*, 2019). Water clusters are able to act as anion transport channels within the AEMs, improving hydroxide conductivity (Zhang *et al.*, 2013).

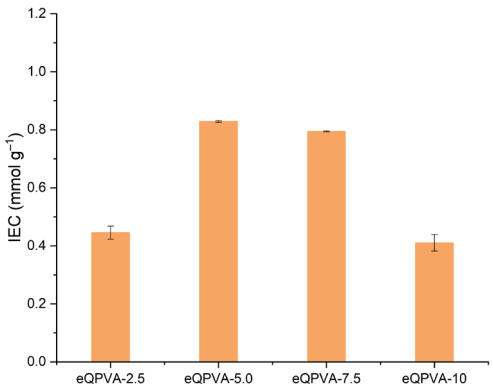

Fig. 6 Ion Exchange capacity of eQPVA-x AEMs.

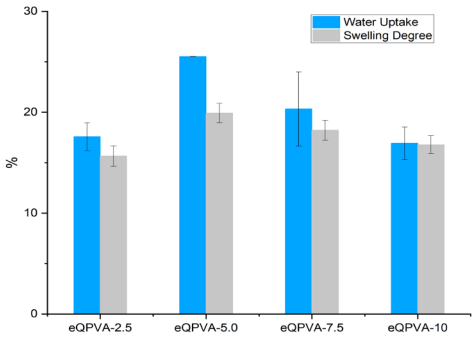

Fig. 7 Sweling properties of eQPVA-x AEMs.

At low water content or low hydration level and in alkaline conditions, OH^- ions can react with side cation charge groups, which lessen the IEC of AEMs since only free ions play a part in the conductivity. Furthermore, the degradation of the cation charge groups will reduce the performance and lifetime of the AEMs (Tomasino *et al.*, 2022). In addition to the lack of hydration, excessive water content is also avoided in AEMs. This excessive water content can induce severe swelling, which can cause instability in the membrane dimensions causing mechanical degradation. Moreover, the excessive water content may dissolve some of the charged cations bound in the polymer backbone, lowering the IEC and causing the anionic conductivity to decrease (Vandiver *et al.*, 2014; Zheng *et al.*, 2018).

The water uptake (WU) and swelling degree (SD) of eQPVA-x AEMs are depicted in Figure 7. The AEM with the lowest QPVA matrix concentration (eQPVA-2.5) has a water uptake of 17.6 wt.%. By incorporating QPVA 5 wt.% (eQPVA-5.0), the WU increases by 45% to 25.5 wt. %. However, by further increasing the concentration of the matrix to 7.5 (eQPVA-7.5) and 10.0 wt.% (eQPVA-10.0), the WU decrease to 20.3 and 16.9 wt.%. The results of the WU are in accordance with the IEC values. Change in water uptake is significantly connected to the amount of cation groups attached to the AEMs, which in the case of these eQPVA-x membranes, are quaternary ammonium groups from QPVA (Samsudin *et al.*, 2021). The swelling degree measurement demonstrates a similar tendency to water uptake. The higher the water uptake indicates the higher the water content in the membrane, which leads to swelling formation and results in changes in the dimensions of the membrane.

3.5 Hydroxide Conductivity

Hydroxide conductivity is the most crucial characteristic of AEMs, owing to the principal role of AEMs as OH^- ions conductors. The conductivity of AEMs is very reliant on the WU and IEC of the AEMs. The high hydrophilicity of the anion exchange membranes is resulted from the high density of cation charge groups within the AEMs, which provide sufficient anionic conductivity (Ayaz *et al.*, 2022). Figure 8 exhibits the hydroxide conductivity of eQPVA-x AEMs. The eQPVA-x AEMs demonstrate OH^- conductivities in the range of 0.71–2.26 mS cm^{-1} at 30 °C. Generally, the AEMs with the highest IEC and WU also possess the highest hydroxide conductivity, which can also be observed in this work. The eQPVA-5.0 exhibits the highest value of WU and IEC, which also demonstrates the highest OH^- conductivity of 2.26 mS cm^{-1}. The Grotthuss mechanism describes how the hydroxide ions migrate along the water molecules chain via the formation and breaking of hydrogen bonds (Li *et al.*, 2020). Accordingly, as WU increases, water content rises as well, improving the conductivity of hydroxide ions.

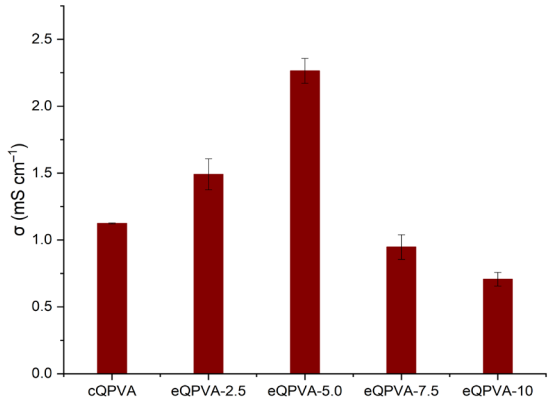

Fig. 8 Hydroxide conductivity of eQPVA-x AEMs.

High hydroxide conductivity has a favorable impact on power density and is accountable for reduced power/ohmic losses (Cermenek *et al.*, 2018). The higher the ionic conductivity, the more hydroxide ions are transported through the membrane so that more hydroxide ions react with the fuel to produce more electrons. The increase in electrons leads to an increase in the current density, which follows equation 5 (Kang & Cannon, 2015).

$$I = \sigma E \quad (5)$$

Where I is current density, σ is conductivity and E is electric field.

Since power density (P) is the multiplication of current density (I) and voltage (V) according to equation 6, an increase in current density will give a proportional increase in power density (O'Hayre, 2017).

$$P = VI \quad (6)$$

This is consistent with a study conducted by Samsudin *et al.* (2021, 2022) that membranes of different conductivity will produce different power densities in the same fuel cell and operating conditions.

4. Conclusion

Anion exchange membranes (AEMs) composed of Gohsenx™ K-434 quaternary ammonium poly(vinyl alcohol) (PVA) as material for electrospun fiber mats and inter-fiber void filler have been prepared by the electrospinning method. FTIR spectra recognized the primary functional groups of membranes. SEM images display the electrospun nanofibers structures of eQPVA with a mean size of 100.96 nm and the surface morphology of eQPVA-5.0 dense AEMs. By incorporating the QPVA matrix of 5 wt.% concentration, the eQPVA-5.0 membrane achieved the highest IEC, water uptake, swelling degree, and hydroxide conductivity of 0.82 mmol g^{-1}, 25.5%, 19.9%, and 2.26 ms cm^{-1}, respectively.

Acknowledgments

The authors thank the Austrian Science Fund (FWF) for providing financial support for the study under project number I 3871-N37. Additionally, the authors acknowledge Kemdikbud (Indonesia) and OeAD (Austria) for the IASP scholarship.

Author Contributions: A.M.S.: Conceptualization, methodology, formal analysis, writing—original draft, writing—review and editing, V.H.; writing—review and editing, supervision, resources, project administration. All authors have read and agreed to the published version of the manuscript.

Funding: This research was funded by Austrian Science Fund (FWF) under project number I 3871-N37.

Conflicts of Interest: The authors declare no conflict of interest.

References

Aslam, M., Kalyar, M. A., & Raza, Z. A. (2018). Polyvinyl alcohol: A review of research status and use of polyvinyl alcohol based nanocomposites. *Polymer Engineering and Science*, *58*(12), 2119–2132. https://doi.org/10.1002/pen.24855

Ayaz, S., Yao, Z. Y., Chen, Y. J., & Yu, H. Y. (2022). Preparation of poly(arylene ether ketone) based anion exchange membrane with pendant pyrimidinium and pyridazinium cation derivatives for alkaline fuel cell. *Journal of Membrane Science*, *659*(June), 120778. https://doi.org/10.1016/j.memsci.2022.120778

Becerra-Arciniegas, R. A., Narducci, R., Ercolani, G., Antonaroli, S., Sgreccia, E., Pasquini, L., Knauth, P., & Di Vona, M. L. (2019). Alkaline stability of model anion exchange membranes based on poly(phenylene oxide) (PPO) with grafted quaternary ammonium groups: Influence of the functionalization route. *Polymer*, *185*, 121931. https://doi.org/10.1016/j.polymer.2019.121931

Cermenek, B., Ranninger, J., & Hacker, V. (2018). Alkaline direct ethanol fuel cell. In *Ethanol: Science and Engineering* (pp. 383–405). Elsevier. https://doi.org/10.1016/B978-0-12-811458-2.00015-8

Das, G., Choi, J.-H., Nguyen, P. K. T., Kim, D.-J., & Yoon, Y. S. (2022). Anion Exchange Membranes for Fuel Cell Application: A Review. *Polymers*, *14*(6), 1197. https://doi.org/10.3390/polym14061197

Ding, C., & Qiao, Z. (2022). A review of the application of polyvinyl alcohol membranes for fuel cells. *Ionics*, *28*(1), 1–13. https://doi.org/10.1007/s11581-021-04338-w

Du, S., Li, S., Xie, N., Xu, Y., Weng, Q., Ning, X., Chen, P., Chen, X., & An, Z. (2022). Development of rigid side-chain poly(ether sulfone)s based anion exchange membrane with multiple annular quaternary ammonium ion groups for fuel cells. *Polymer*, *251*(April), 124919. https://doi.org/10.1016/j.polymer.2022.124919

Du, X., Zhang, H., Yuan, Y., & Wang, Z. (2020). Semi-interpenetrating network anion exchange membranes based on quaternized polyvinyl alcohol/poly(diallyldimethylammonium chloride). *Green Energy and Environment*. 6(5), 743-750 https://doi.org/10.1016/j.gee.2020.06.015

Elumalai, V., Ganesh, T., Selvakumar, C., & Sangeetha, D. (2018). Phosphonate Ionic Liquid Immobilised SBA-15/SPEEK Composite Membranes for High Temperature Proton Exchange Membrane Fuel Cells. *Materials Science for Energy Technologies*. https://doi.org/10.1016/j.mset.2018.08.003

Feketefoldi, B., & Cermenek, B. (2016). Chitosan-Based Anion Exchange Membranes for Direct Ethanol Fuel Cells. *Journal of Membrane Science & Technology*, *06*(01), 1–9. https://doi.org/10.4172/2155-9589.1000145

Fennessey, S. F., & Farris, R. J. (2004). Fabrication of aligned and molecularly oriented electrospun polyacrylonitrile nanofibers and the mechanical behavior of their twisted yarns. *Polymer*, *45*, 4217–4225. https://doi.org/10.1016/j.polymer.2004.04.001

Francia, C., Ijeri, V. S., Specchia, S., & Spinelli, P. (2011). Estimation of hydrogen crossover through Nafion® membranes in PEMFCs. *Journal of Power Sources*, *196*(4), 1833–1839. https://doi.org/10.1016/j.jpowsour.2010.09.058

Gong, Y., Liao, X., Xu, J., Chen, D., & Zhang, H. (2016). Novel anion-conducting interpenetrating polymer network of quaternized polysulfone and poly(vinyl alcohol) for alkaline fuel cells. *International Journal of Hydrogen Energy*, *41*(13), 5816–5823. https://doi.org/10.1016/j.ijhydene.2016.02.037

Guo, M., Ban, T., Wang, Y., Wang, Y., Zhang, Y., Zhang, J., & Zhu, X. (2022). Exploring highly soluble ether-free polybenzimidazole as anion exchange membranes with long term durability. *Journal of Membrane Science*, *647*(January), 120299. https://doi.org/10.1016/j.memsci.2022.120299

Hagesteijn, K. F. L., Jiang, S., & Ladewig, B. P. (2018). A review of the synthesis and characterization of anion exchange membranes. *Journal of Materials Science*. 53, 11131–11150; https://doi.org/10.1007/s10853-018-2409-y

Huang, J., Yu, Z., Tang, J., Wang, P., Tan, Q., Wang, J., & Lei, X. (2022). A review on anion exchange membranes for fuel cells: Anion-exchange polyelectrolytes and synthesis strategies. *International Journal of Hydrogen Energy*, *47*(65), 27800–27820. https://doi.org/10.1016/j.ijhydene.2022.06.140

Huang, T., Qiu, X., Zhang, J., Li, X., Pei, Y., Jiang, H., Yue, R., Yin, Y., Jiang, Z., Zhang, X., & Guiver, M. D. (2022). Hydrogen crossover through microporous anion exchange membranes for fuel cells. *Journal of Power Sources*, *527*, 231143. https://doi.org/10.1016/j.jpowsour.2022.231143

Inaba, M., Kinumoto, T., Kiriake, M., Umebayashi, R., Tasaka, A., & Ogumi, Z. (2006). Gas crossover and membrane degradation in polymer electrolyte fuel cells. *Electrochimica Acta*, *51*(26), 5746–5753. https://doi.org/10.1016/j.electacta.2006.03.008

Iravaninia, M., & Rowshanzamir, S. (2015). Polysulfone-based Anion Exchange Membranes for Potential Application in Solid Alkaline Fuel Cells. *Journal of Renewable Energy and Environment*, *2*(2), 59–65. https://doi.org/10.30501/jree.2015.70071

Kang, W., & Cannon, J. L. (2015). A membrane-based electro-separation method (MBES) for sample clean-up and norovirus concentration. *PLoS ONE*, *10*(10), 1–22. https://doi.org/10.1371/journal.pone.0141484

Kumar, P., Bharti, R. P., Kumar, V., & Kundu, P. P. (2018). Polymer electrolyte membranes for microbial fuel cells: Part a. nafion-based membranes. In *Progress and Recent Trends in Microbial Fuel Cells* (pp. 47–72). Elsevier B.V. https://doi.org/10.1016/B978-0-444-64017-8.00004-X

Li, Y., Li, M., Zhou, S., Xue, A., Zhang, Y., Zhao, Y., Zhong, J., Zhang, Q., & Yang, D. (2020). Enhancement of hydroxide conductivity by incorporating nanofiber-like palygorskite into quaternized polysulfone as anion exchange membranes. *Applied Clay Science*, *195*(June), 105702. https://doi.org/10.1016/j.clay.2020.105702

Mayadevi, T. S., Min, K., Choi, O., Chae, J. E., Kim, H. J., Choi, C. H., Kang, H., Park, C. H., & Kim, T. H. (2022). PPOs having piperidinium-based conducting head groups with extra molecular interaction sites as new anion exchange membranes. *International Journal of Hydrogen Energy*, *47*(36), 16222–16234. https://doi.org/10.1016/j.ijhydene.2022.03.110

Movil, O., Frank, L., & Staser, J. A. (2015). Graphene Oxide-Polymer Nanocomposite Anion-Exchange Membranes. *Journal of the Electrochemical Society*, *162*(4), F419–F426. https://doi.org/10.1149/2.0681504jes

O'Hayre, R. P. (2017). Fuel cells for electrochemical energy conversion. *EPJ Web of Conferences*, *148*, 1–16. https://doi.org/10.1051/epjconf/201714800013

Patel, A., Patra, F., Shah, N., & Khedkar, C. (2018). Application of Nanotechnology in the Food Industry: Present Status and Future Prospects. In *Impact of Nanoscience in the Food Industry* (pp. 1–27). Elsevier Inc. https://doi.org/10.1016/B978-0-12-811441-4.00001-7

Ramaswamy, N., & Mukerjee, S. (2020). Alkaline Anion-Exchange Membrane Fuel Cells : Challenges in Electrocatalysis and Interfacial Charge Transfer. *Chem. Rev.*, *119*, 11945–11979. https://doi.org/10.1021/acs.chemrev.9b00157

Samsudin, A. M., Bodner, M., & Hacker, V. (2022). A Brief Review of Poly (Vinyl Alcohol) -Based Anion Exchange Membranes for Alkaline Fuel Cells. *Polymer*, *14*, 3565. https://doi.org/10.3390/polym14173565

Samsudin, A. M., & Hacker, V. (2019). Preparation and characterization of PVA/PDDA/nano-zirconia composite anion exchange membranes for fuel cells. *Polymers*, *11*, 1399. https://doi.org/10.3390/polym11091399

Samsudin, A. M., & Hacker, V. (2021). Effect of Crosslinking on the Properties of QPVA/PDDA Anion Exchange Membranes for Fuel Cells Application. *Journal of The Electrochemical Society*, *168*, 044526. https://doi.org/10.1149/1945-7111/abf781

Samsudin, A. M., Roschger, M., Wolf, S., & Hacker, V. (2022). Preparation and Characterization of QPVA/PDDA Electrospun Nanofiber Anion Exchange Membranes for Alkaline Fuel Cells. *Nanomaterials*, *12*(22), 3965. https://doi.org/10.3390/nano12223965

Samsudin, A. M., Wolf, S., Roschger, M., & Hacker, V. (2021). Poly(vinyl alcohol)-based Anion Exchange Membranes for Alkaline Polymer Electrolyte Fuel Cells. *International Journal of Renewable Energy Development*, *10*(3), 435–443. https://doi.org/10.14710/ijred.2021.33168

Sood, R., Cavaliere, S., Jones, D. J., & Rozière, J. (2016). Electrospun nanofibre composite polymer electrolyte fuel cell and electrolysis membranes. *Nano Energy*, *26*, 729–745. https://doi.org/10.1016/j.nanoen.2016.06.027

Susanto, H., Samsudin, A. M., Faz, M. W., & Rani, M. P. H. (2016). Impact of post-treatment on the characteristics of electrospun poly (vinyl alcohol)/chitosan nanofibers. In H. Susanto, R. Suryana, & K. Triyana (Eds.), *AIP Conference Proceedings* (Vol. 1725, p. 020087). AIP Publishing LLC. https://doi.org/10.1063/1.4945541

Tamura, T., & Kawakami, H. (2010). Aligned Electrospun Nanofiber Composite Membranes for Fuel Cell Electrolytes. *Nano Letters*, *10*, 1324–1328. https://doi.org/10.1021/nl1007079

Tomasino, E., Mukherjee, B., Ataollahi, N., & Scardi, P. (2022). Water Uptake in an Anion Exchange Membrane Based on Polyamine: A First-Principles Study. *The Journal of Physical Chemistry B*, *126*(38), 7418–7428. https://doi.org/10.1021/acs.jpcb.2c04115

Vandiver, M. A., Caire, B. R., Carver, J. R., Waldrop, K., Hibbs, M. R., Varcoe, J. R., Herring, A. M., & Liberatore, M. W. (2014). Mechanical Characterization of Anion Exchange Membranes by Extensional Rheology under Controlled Hydration. *Journal of The Electrochemical Society*, *161*(10), H677–H683. https://doi.org/10.1149/2.0971410jes

Wang, Y.-J., Qiao, J., Baker, R., & Zhang, J. (2013). Alkaline polymer electrolyte membranes for fuel cell applications. *Chemical Society Reviews*, *42*(13), 5768–5787. https://doi.org/10.1039/c3cs60053j

Wang, Z., Zhou, S. F., Zhuo, Y. Z., Lai, A. N., Lu, Y. Z., & Wu, X. Bin. (2022). Adamantane-based block poly(arylene ether sulfone)s as anion exchange membranes. *Polymer*, *255*(July), 125155. https://doi.org/10.1016/j.polymer.2022.125155

Yang, J. M., Fan, C. S., Wang, N. C., & Chang, Y. H. (2018). Evaluation of membrane preparation method on the performance of alkaline polymer electrolyte: Comparison between poly(vinyl alcohol)/chitosan blended membrane and poly(vinyl alcohol)/chitosan electrospun nanofiber composite membranes. *Electrochimica Acta*, *266*, 332–340. https://doi.org/10.1016/j.electacta.2018.02.043

Zelovich, T., Vogt-Maranto, L., Hickner, M. A., Paddison, S. J., Bae, C., Dekel, D. R., & Tuckerman, M. E. (2019). Hydroxide Ion Diffusion in Anion-Exchange Membranes at Low Hydration: Insights from Ab Initio Molecular Dynamics. *Chemistry of Materials*, *31*(15), 5778–5787. https://doi.org/10.1021/acs.chemmater.9b01824

Zhang, G., Li, R., Wang, X., Chen, X., Shen, Y., & Fu, Y. (2022). The inhibiting water uptake mechanism of main-chain type N-spirocyclic quaternary ammonium ionene blended with polybenzimidazole as anion exchange membrane. *Separation and Purification Technology*, *291*(January), 120950. https://doi.org/10.1016/j.seppur.2022.120950

Zhang, J., Qiao, J., Jiang, G., Liu, L., & Liu, Y. (2013). Cross-linked poly(vinyl alcohol)/poly (diallyldimethylammonium chloride) as anion-exchange membrane for fuel cell applications. *Journal of Power Sources*, *240*, 359–367. https://doi.org/10.1016/j.jpowsour.2013.03.162

Zheng, Y., Ash, U., Pandey, R. P., Ozioko, A. G., Ponce-González, J., Handl, M., Weissbach, T., Varcoe, J. R., Holdcroft, S., Liberatore, M. W., Hiesgen, R., & Dekel, D. R. (2018). Water Uptake Study of Anion Exchange Membranes. *Macromolecules*, *51*(9), 3264–3278. https://doi.org/10.1021/acs.macromol.8b00034